
Proceedings Paper:
Radhakrishnan, Vignesh, Ellison, Peter John, Patil, Samadhan Bhaulal et al. (2023) Determining bone position from wearable antennas using microwave imaging: A feasibility study. In: URSI GASS 2023, proceedings. URSI General Assembly and Scientific Symposium 2023, 19-26 Aug 2023 URSI General Assembly and Scientific Symposium. IEEE, JPN.

https://doi.org/10.23919/URSIGASS57860.2023.10265389

URSI GASS 2023, Sapporo, Japan, 19 – 26 August 2023

Determining bone position from wearable antennas using microwave imaging: A feasibility study

Vignesh Radhakrishnan*(1), Peter Ellison (1), Samadhan Patil (1), Adar Pelah (1), Martin Robinson (1)
(1) School of Physics, Engineering and Technology, University of York, UK
e-mail: vignesh.radhakrishnan@york.ac.uk

Abstract

Imaging of the bone is an important clinical tool in detecting fractures, determining loss of bone density and in improving movement and gait analysis, with visualisation predominantly performed using ionising imaging. Microwave imaging, an alternative non-ionising imaging modality, has shown promising results in analysing bone density variation and in determining the presence of tears in joint tissues. In this study, we aimed to detect the location of the bone in the leg using radar-based microwave imaging. Confocal imaging algorithms were applied to scattering data acquired from simulated wearable antennas on a male human model without the use of a coupling liquid. We successfully detected both thigh and shin bones, with a localisation error of 2.5 cm, 0.91 cm and 1.34 cm for the femur, tibia and fibula centres respectively. Notably, these errors are in line with tumour detection errors. Our methodology and results illustrate a safe, easy-to-implement and simple pipeline using off-the-shelf antennas and algorithms to determine bone position using wearable sensors. We believe this technique has wide ranging applications, particularly in improving the accuracy of clinical movement analysis systems.

1 Introduction

Visualising the interior of the human body is an important aspect of many clinical studies. Imaging of both healthy and abnormal tissues is used to gain a deeper understanding of the human anatomy and the physiology of pathologies [1]. Applications of imaging include the detection of bone fractures, tumours, strokes, and the visualisation of bone angles during movement [2], [3]. Clinical skin-mounted marker based motion capture systems use the bone's exact position and orientation during movement to reduce soft tissue artefacts, a critical source of marker error caused by the movement of underlying soft tissues [2], [4]. Soft tissue artefacts can result in marker position errors up to 4 cm, affecting the clinical usability of the systems [5]. Fluoroscopy, an ionising modality of imaging, is frequently used to visualise the bones during movement. These images are subsequently used to determine the magnitude of soft tissue artefacts or project skin-markers onto the bone: one potential method to reduce soft tissue artefacts[6], [7]. However, the use of fluoroscopy is hindered by its high cost, complexity of the system and its ionising nature [2], [3].

Microwave imaging is a low cost, non-ionising imaging modality alternative, whose application in detecting breast tumours, identifying strokes and in analysing variation in bone density has been previously researched [8]–[10]. Microwave imaging of the human body can be grouped into two categories: tomography imaging, which provides a map of the distribution of various tissues with their electrical properties, and radar-based imaging, which provides the location of a strong scatterer based on dielectric contrast between the object of interest and surrounding tissues [1]. Bone imaging is primarily performed using tomography methods, where differences in dielectric properties between healthy and pathological bones, or between healthy and torn joint tissues, are visualised [11]. Radar-based methods, on the other hand, are typically applied in tumour detection, where the dielectric contrast between the tumour and surrounding tissues is exploited [10]. To our knowledge, only one study has evaluated radar-based methods for bone detection [12]. Specifically, the authors in question acquired scattering parameters from antennas immersed in a coupling liquid, and determined the bone position of a multi-layered phantom using a noncoherent imaging algorithm [12].

In this study we aim to evaluate the efficacy of a simple, easy-to-implement pipeline to determine the accurate location of the bones relative to the superficial tissue using microwave imaging through:

1) The use of wearable antennas without the need of coupling liquid
2) Applying a confocal imaging algorithm to determine the location of the bone
3) Applying the imaging algorithm without the need for a reference scan or empty scan subtraction

To the best of our knowledge, this is the first study evaluating the use of microwave imaging to calculate bone location using wearable antennas. We believe this pipeline has the potential to be integrated with clinical movement analysis systems to reduce soft tissue artefacts.

2 Methods

2.1 Simulation

In order to evaluate the feasibility of determining bone position from microwave imaging using wearable antennas, five broadband antennas [13] tuned at f=0.9 GHz were modelled in Sim4Life [14]. The resonant wave half-

dipole antenna, D900V2, has an overall length of 147.5 mm and was chosen due to its simple design and prior application with body-mimicking liquids [13]. The five antennas were placed around the thigh and shin of a virtual population model, Duke (Figure 1). Scattering parameters were calculated and recorded through a multiport simulation, implemented using the finite-difference time-domain solver in Sim4Life, with a Gaussian pulse centred at 0.9 GHz and bandwidth of 1 GHz provided as input to each antenna. All tissues in the Duke model (skin, muscle, fat and bone) were assigned dielectric properties based on the IT'IS database provided by Sim4Life [14]. Antenna locations, bone locations, and the distance between the antennas and the bone were calculated in Sim4Life.

a) b)

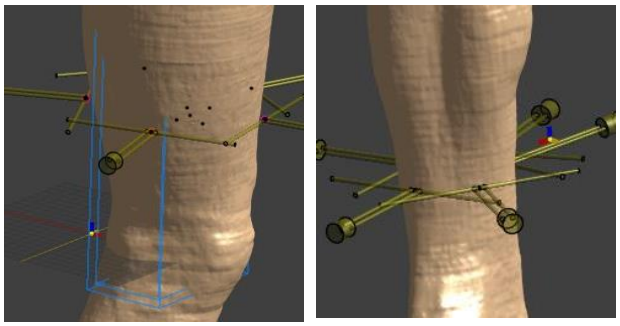

Figure 1. a) Half-wave dipole antennas placed around the thigh of the virtual population model, Duke. **b)** Half-wave dipole antennas placed around the shin of the virtual population model, Duke.

2.2 Microwave imaging

Confocal imaging algorithms implemented in the Microwave Radar-based Imaging Toolbox (MERIT) [15] were applied to the scattering data. In particular the delay-multiply-and-sum algorithm (DMAS) [16] and modified delay-and-sum (MDAS) [17] were applied to the transmission scattering parameters, with a 2d transversal slice at the antenna locations computed as the imaging domain. The bones were identified as pixels, with the maximum intensity value in the reconstructed image indicating a region of high scattering due to dielectric contrast between bone and muscle. Localisation error (LE), defined as the euclidean distance between the centroid of the bone in the reconstructed image and centroid of the bone position estimated using Sim4life, was calculated for each image. Confocal imaging algorithms were additionally applied to two breast-tumour detection datasets provided in the toolbox, to validate the accuracy of the algorithms [15].

3 Results

The femur, fibula and tibia were successfully detected (Figures 2 and 3). Centroid of the femur in the reconstructed image was located at (11.62 cm, 0.82 cm) with the centroids of fibula and tibia detected at (7.29 cm, -0.17 cm) and (9.29 cm, 1.57 cm), respectively.

Localisation error for the femur, tibia, fibula and two breast-tumour datasets are shown in Table 1.

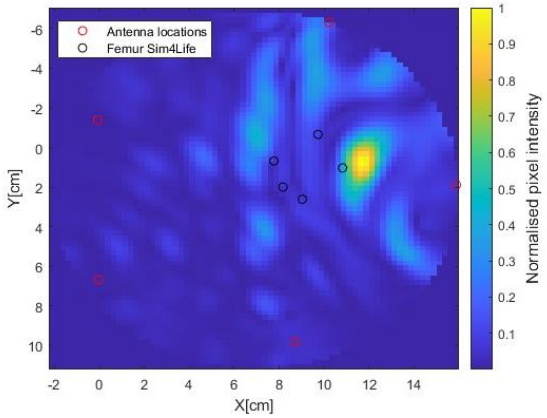

Figure 2. Reconstructed image showing the femur located at (11.62 cm, 0.82 cm). Imaged femur is identified as pixels with high intensity values. The black circles indicate the surface of the femur as calculated in Sim4Life. Red circles show the centres of the dipole antennas.

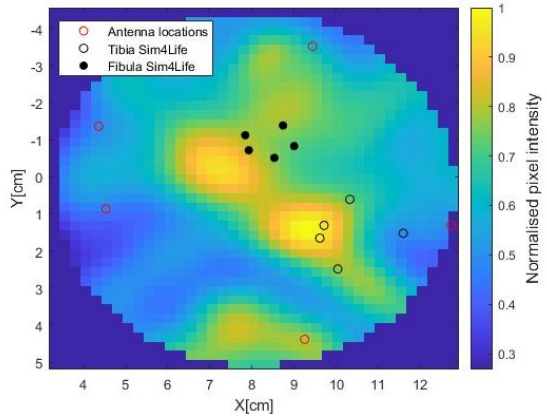

Figure 3. Reconstructed image of the tibia and fibula located at (9.29 cm, 1.57 cm) and (7.29 cm, -0.17 cm), respectively. The imaged tibia and fibula are identified as pixels with high intensity values. The black and white circles indicate the surface of the tibia and fibula respectively, as calculated by Sim4Life. The red circles show the centres of the dipole antennas.

Table 1. Localisation error for femur, tibia, fibula and the two breast-tumour datasets.

Data	Location in image (cm)	Actual location (cm)	Error (cm)
Femur	(11.6, 0.8)	(9.1, 1.1)	2.5
Tibia	(9.3, 1.6)	(10.2, 1.5)	0.9
Fibula	(7.3, -0.2)	(8.4, -0.9)	1.3
Breast 1-B0_P3 [15]	(0.5, 0.2)	(1.5, 0.0)	1.0
Breast 2-B0_P5 [15]	(0.5, 0.2)	(1.5, 0.0)	1.0

4 Discussion and Conclusion

Mapping the accurate position and orientation of the bone during movement and gait analysis is crucial for clinical diagnosis of pathologies and rehabilitation. Data acquired from clinical skin-mounted marker based systems are affected by soft tissue artefacts, with errors up to 4cm, which may invalidate their clinical useability [4], [5]. To reduce these artefacts, complementary methods of determining bone position using ionising imaging have been increasingly implemented [2], [3]. Despite the accuracy of these methods, the subjects were exposed to ionisation equivalent to four years of natural background radiation [2].

In this study we have illustrated a novel, non-ionising method of determining bone position. Our results indicate that bone position can be successfully determined using wearable antennas and microwave imaging. The femur, tibia and fibula were located with errors of 2.5, 0.9 and 1.3 cm respectively. The variation in errors may be caused due to the distance of the bone from the skin, with the femur having the maximum error and located furthest away from the skin, with the inverse true for the tibia. Furthermore, our results indicate that radar-based imaging is feasible, even without the use of a coupling liquid. Microwave imaging predominantly uses antennas immersed in a coupling liquid with dielectric properties similar to the object being imaged to reduce the scattering at the air-skin interface. Whilst the use of coupling liquid may reduce localisation error, imaging setups with coupling liquids are less viable in dynamic applications such as movement analysis.

We achieved a low localisation error, less than or similar to results obtained in breast tumour detection[18], however the error could be reduced by changing the imaging algorithm and altering the antenna design. Whilst the confocal imaging algorithms we used in this study, DMAS and MDAS (versions of the classic delay-and-sum beamformer), have been applied extensively in the detection of breast-tumours — due to their superior clutter suppression compared to other confocal imaging algorithms — they still suffer from false positives and relatively low signal-to-mean ratio [10], [16], [19]. Confocal imaging algorithms are also negatively affected by the frequency dispersion of tissues and the influence of tissues at close proximity to the antennas, which affects their frequency response. These are further exacerbated when imaging the bone due to the heterogeneity of the background tissues [20]. The application of imaging algorithms, such as interferometric multiple signal classification, wideband multiple signal classification and noncoherent migration may improve the accuracy of bone detection. Care must be taken when applying imaging techniques, as they were primarily designed to detect point scatterers, which is the case in breast-tumour detection.

The design of antennas strongly influences the accuracy of bone detection. Whilst the resonant wave half-dipole antenna used in this study has provided sufficient penetration for bone detection, the penetration and coupling of power into the body could be improved through antenna design. Antenna designs incorporating metamaterials [9], a coupling-structure [21] or novel-power split devices [8] have been proposed, which could provide both enhanced penetration and form-factor for wearable applications.

Through this study we have demonstrated a safe, simple, and easy-to-implement pipeline for determining bone location relative to the skin using wearable sensors. Whilst the localisation error can be further improved using novel imaging techniques and enhanced antenna design, our results indicate the feasibility of bone detection using off-the-shelf antennas and imaging algorithms. We believe this technique, with compact and lightweight wearable antennas, has the potential to improve the precision of clinical movement analysis without the need for ionising bone imaging. The antennas would enable a non-ionising method of determining bone position with the absolute position of antennas provided by marker based systems.

Acknowledgements

The authors would like to thank ZMT Zurich MedTech AG (www.zmt.swiss, accessed Jan. 23, 2023) for having provided their simulation software Sim4Life.

References

[1] R. Chandra, H. Zhou, I. Balasingham, and R. M. Narayanan, “On the Opportunities and Challenges in Microwave Medical Sensing and Imaging,” *IEEE Trans. Biomed. Eng.*, vol. 62, no. 7, pp. 1667–1682, Jul. 2015, doi: 10.1109/TBME.2015.2432137.

[2] N. M. Fiorentino, P. R. Atkins, M. J. Kutschke, K. Bo Foreman, and A. E. Anderson, “Soft tissue artifact causes underestimation of hip joint kinematics and kinetics in a rigid-body musculoskeletal model,” *J. Biomech.*, vol. 108, p. 109890, Jul. 2020, doi:

10.1016/j.jbiomech.2020.109890.
[3] W. R. Taylor *et al.*, “A comprehensive assessment of the musculoskeletal system: The CAMS-Knee data set,” *J. Biomech.*, vol. 65, pp. 32–39, Dec. 2017, doi: 10.1016/j.jbiomech.2017.09.022.
[4] A. Leardini, L. Chiari, U. Della Croce, and A. Cappozzo, “Human movement analysis using stereophotogrammetry. Part 3. Soft tissue artifact assessment and compensation,” *Gait Posture*, vol. 21, no. 2, pp. 212–225, Feb. 2005, doi: 10.1016/j.gaitpost.2004.05.002.
[5] A. Peters, B. Galna, M. Sangeux, M. Morris, and R. Baker, “Quantification of soft tissue artifact in lower limb human motion analysis: a systematic review,” *Gait Posture*, vol. 31, no. 1, pp. 1–8, Jan. 2010, doi: 10.1016/j.gaitpost.2009.09.004.
[6] M. Begon, C. Bélaise, A. Naaim, A. Lundberg, and L. Chèze, “Multibody kinematics optimization with marker projection improves the accuracy of the humerus rotational kinematics,” *J. Biomech.*, vol. 62, pp. 117–123, Sep. 2017, doi: 10.1016/j.jbiomech.2016.09.046.
[7] M. A. Masum, M. R. Pickering, A. J. Lambert, J. M. Scarvell, and P. N. Smith, “Multi-slice ultrasound image calibration of an intelligent skin-marker for soft tissue artefact compensation,” *J. Biomech.*, vol. 62, pp. 165–171, Sep. 2017, doi: 10.1016/j.jbiomech.2016.12.030.
[8] S. N. Makarov, G. M. Noetscher, S. Arum, R. Rabiner, and A. Nazarian, “Concept of a Radiofrequency Device for Osteopenia/Osteoporosis Screening,” *Sci. Rep.*, vol. 10, no. 1, p. 3540, Feb. 2020, doi: 10.1038/s41598-020-60173-5.
[9] M. S. Islam, M. T. Islam, and A. F. Almutairi, “A portable non-invasive microwave based head imaging system using compact metamaterial loaded 3D unidirectional antenna for stroke detection,” *Sci. Rep.*, vol. 12, no. 1, p. 8895, May 2022, doi: 10.1038/s41598-022-12860-8.
[10] M. A. Elahi *et al.*, “Evaluation of Image Reconstruction Algorithms for Confocal Microwave Imaging: Application to Patient Data,” *Sensors* , vol. 18, no. 6, May 2018, doi: 10.3390/s18061678.
[11] S. M. Salvador, E. C. Fear, M. Okoniewski, and J. R. Matyas, “Exploring Joint Tissues With Microwave Imaging,” *IEEE Trans. Microw. Theory Tech.*, vol. 58, no. 8, pp. 2307–2313, Aug. 2010, doi: 10.1109/TMTT.2010.2052662.
[12] G. Ruvio, A. Cuccaro, R. Solimene, A. Brancaccio, B. Basile, and M. J. Ammann, “Microwave bone imaging: a preliminary scanning system for proof-of-concept,” *Healthc Technol Lett*, vol. 3, no. 3, pp. 218–221, Sep. 2016, doi: 10.1049/htl.2016.0003.
[13] “V&V Dipoles (>300 MHz) » SPEAG, Schmid & Partner Engineering AG.” https://speag.swiss/components/emv-and-v-sources/sar/v-and-v-dipoles-300-mhz/ (accessed Jan. 22, 2023).
[14] “SIM4LIFE » zurich med tech.” https://zmt.swiss/sim4life/ (accessed Jan. 23, 2023).
[15] D. O’Loughlin *et al.*, “Open-source software for microwave radar-based image reconstruction,” pp. 1–4, Apr. 2018, doi: 10.1049/cp.2018.0767.
[16] H. Been Lim, N. Thi Tuyet Nhung, E.-P. Li, and N. Duc Thang, “Confocal Microwave Imaging for Breast Cancer Detection: Delay-Multiply-and-Sum Image Reconstruction Algorithm,” *IEEE Transactions on Biomedical Engineering*, vol. 55, no. 6, pp. 1697–1704, Jun. 2008, doi: 10.1109/TBME.2008.919716.
[17] M. Klemm, J. A. Leendertz, D. Gibbins, I. J. Craddock, A. Preece, and R. Benjamin, “Microwave Radar-Based Breast Cancer Detection: Imaging in Inhomogeneous Breast Phantoms,” *IEEE Antennas Wirel. Propag. Lett.*, vol. 8, pp. 1349–1352, 2009, doi: 10.1109/LAWP.2009.2036748.
[18] G. Ruvio, R. Solimene, A. Cuccaro, D. Gaetano, J. E. Browne, and M. J. Ammann, “Breast cancer detection using interferometric MUSIC: experimental and numerical assessment,” *Med. Phys.*, vol. 41, no. 10, p. 103101, Oct. 2014, doi: 10.1118/1.4892067.
[19] T. Reimer and S. Pistorius, “An Optimization-Based Approach to Radar Image Reconstruction in Breast Microwave Sensing,” *Sensors* , vol. 21, no. 24, Dec. 2021, doi: 10.3390/s21248172.
[20] A. Cuccaro, A. Dell’Aversano, G. Ruvio, J. Browne, and R. Solimene, “Incoherent Radar Imaging for Breast Cancer Detection and Experimental Validation against 3D Multimodal Breast Phantoms,” *J. Imaging Sci. Technol.*, vol. 7, no. 2, Feb. 2021, doi: 10.3390/jimaging7020023.
[21] D. O. Rodriguez-Duarte, J. A. T. Vasquez, R. Scapaticci, L. Crocco, and F. Vipiana, “Brick-Shaped Antenna Module for Microwave Brain Imaging Systems,” *IEEE Antennas Wirel. Propag. Lett.*, vol. 19, no. 12, pp. 2057–2061, Dec. 2020, doi: 10.1109/LAWP.2020.3022161.